PLANETARY SCIENCE

First measurements of the radiation dose on the lunar surface

Shenyi Zhang[1,2,3,4], Robert F. Wimmer-Schweingruber[1,5]*, Jia Yu[5†], Chi Wang[1], Qiang Fu[6,7], Yongliao Zou[1], Yueqiang Sun[1,2,4], Chunqin Wang[1,2,4], Donghui Hou[1,2,3,4], Stephan I. Böttcher[5], Sönke Burmeister[5], Lars Seimetz[5], Björn Schuster[5], Violetta Knierim[5], Guohong Shen[1,2,4], Bin Yuan[1,2,4], Henning Lohf[5], Jingnan Guo[5,8,9], Zigong Xu[5], Johan L. Freiherr von Forstner[5], Shrinivasrao R. Kulkarni[5], Haitao Xu[1], Changbin Xue[1], Jun Li[1], Zhe Zhang[10], He Zhang[11], Thomas Berger[12], Daniel Matthiä[12], Christine E. Hellweg[12], Xufeng Hou[13], Jinbin Cao[14], Zhen Chang[1,2,4], Binquan Zhang[1,2,4], Yuesong Chen[1], Hao Geng[1], Zida Quan[1,2,4]

Human exploration of the Moon is associated with substantial risks to astronauts from space radiation. On the surface of the Moon, this consists of the chronic exposure to galactic cosmic rays and sporadic solar particle events. The interaction of this radiation field with the lunar soil leads to a third component that consists of neutral particles, i.e., neutrons and gamma radiation. The Lunar Lander Neutrons and Dosimetry experiment aboard China's Chang'E 4 lander has made the first ever measurements of the radiation exposure to both charged and neutral particles on the lunar surface. We measured an average total absorbed dose rate in silicon of 13.2 ± 1 μGy/hour and a neutral particle dose rate of 3.1 ± 0.5 μGy/hour.

INTRODUCTION

The Moon is the next stepping stone for human space exploration, and several nations have announced plans for its exploration by humans. Space radiation exposure is one of the major risks for astronauts' health (*1*–*3*) as the chronic exposure to galactic cosmic rays (GCRs) may have late health effects such as induction of cataract (*4*), cancer (*5*–*7*), or degenerative diseases of the central nervous system (*8*) or other organ systems (*9*, *10*). Moreover, exposure to large solar particle events (SPEs) in a situation with insufficient shielding may cause severe acute effects (*11*). The exposure to GCR is inevitable but generally contributes a low dose rate compared to the sporadic, unpredictable, but sometimes very intense SPEs in which solar energetic particles are accelerated close to the Sun by solar flares and coronal mass ejections. The nucleonic component of GCR consists mainly of protons (~87%), helium (~12%), and heavier nuclei (~1%) (*12*). These nuclei have very high energy and are therefore highly penetrating. Because of their single charge, protons are only weakly ionizing, and helium nuclei are four times more ionizing per nucleus. The remaining 1% of nuclei are high (H) atomic number (Z) and energy (E) elements (HZE) that contribute to radiation damage disproportionally according to the square of their nuclear charge, Z, resulting in very dense ionization along their tracks. Because of nuclear fragmentation and other complex interactions with matter, their exact effects on humans are uncertain but may be considerable (*13*, *14*).

It appears that there have been no active (i.e., time resolved) measurements of the radiation dose rate on the surface of the Moon until the Chinese Chang'E 4 mission landed in the von Karman crater on the far side of the Moon on 3 January 2019 at 02:26 UTC. During the Apollo missions, astronauts carried dosimeters with them (*15*) to the Moon, but time-resolved radiation data from the surface of the Moon were never reported (*16*). Here, we report radiation dose rate measurements with previously unseen accuracy from the surface of the Moon.

For the assessment of the radiation exposure, the relevant quantities have to be measured by the detector systems: The absorbed dose, *D*, is the ratio of the energy (*E*; usually measured in keV) deposited in a detector and the mass, *m*, of the detector and is expressed in units of Gray (Gy = J/kg). Division by the accumulation time results in the measured dose rate (expressed in Gy/hour). Using a combination of two detectors in coincidence, one measures the distribution of energies deposited in a detector to obtain the linear energy transfer (LET) spectrum [usually in units of keV per micrometer (keV/μm)]. This spectrum is integrated with so-called quality factors, *Q*, used as biological weights to obtain the dose equivalent, *H*, which is expressed in units of Sievert (Sv = J/kg). The exact procedures are defined by the International Commission on Radiation Protection (*17*). Because the human body is not made of silicon, and to make dose, dose rate, and LET measurements more easily comparable to others, one normally converts the values measured in Si to the corresponding quantities in water using a constant dose conversion factor of 1.30 (*18*).

The Lunar Lander Neutrons and Dosimetry (LND) experiment is described in more detail in the literature (*19*), but we summarize the pertinent information here for convenience. The LND is mounted in the payload compartment of the Chang'E 4 lander. The red arrow in Fig. 1 points at the reclosable door that protects LND from the cold lunar nights but is open during lunar daytime. The LND consists of

[1]National Space Science Center, Chinese Academy of Sciences, Beijing, PR China. [2]Beijing Key Laboratory of Space Environment Exploration, Beijing, PR China. [3]University of Chinese Academy of Science, Beijing, PR China. [4]Key Laboratory of Environmental Space Situation Awareness Technology, Beijing, PR China. [5]Institute of Experimental and Applied Physics, Christian-Albrechts-University, Kiel, Germany. [6]National Astronomical Observatories, Chinese Academy of Sciences, Beijing, PR China. [7]Key Laboratory of Lunar and Deep Space Exploration, Chinese Academy of Sciences, Beijing, PR China. [8]University of Science and Technology of China, Hefei, PR China. [9]CAS Center for Excellence in Comparative Planetology, Hefei, PR China. [10]Lunar Exploration and Space Engineering Center, Beijing, PR China. [11]China Academy of Space Technology, Beijing, PR China. [12]German Aerospace Center (DLR), Institute of Aerospace Medicine, Cologne, Germany. [13]18th Research Institute, China Electronics Technology Group Corporation, Tianjin, PR China. [14]BeiHang University, Beijing, PR China.
*Corresponding author. Email: wimmer@physik.uni-kiel.de
†Present address: Bosch Sensortec GmbH, Reutlingen, Germany.

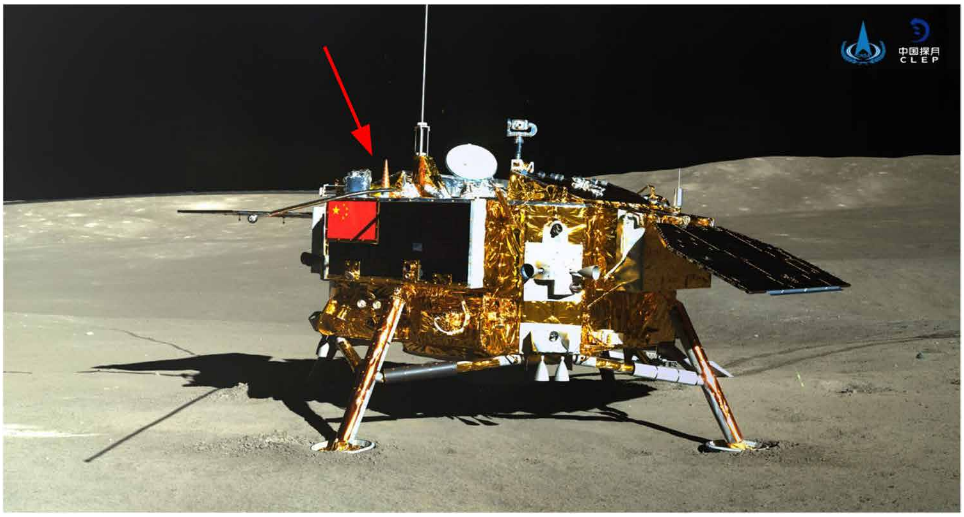

Fig. 1. View of the Chang'E 4 lander with the location of the LND sensor head indicated by the red arrow. LND is mounted in the Chang'E 4 payload compartment; the lid at the tip of the red arrow is closed at night to protect LND from the cold lunar night. Photo credit: Chinese National Space Agency (CNSA) and National Astronomical Observatories of China (NAOC).

a stack of 10 dual-segment silicon solid-state detectors (SSDs), A to J, as shown in the main part of Fig. 2. Total absorbed dose and dose rate are measured in detector B, and the absorbed dose (rate) from neutral particles is measured in the inner segment of the C detector, C1, with the closely spaced detectors B and D as well as the outer segment of C, C2, serving as anticoincidence to discriminate against charged particles. The LET is then determined as discussed above from the *dE/dx* measured using three different combinations of detector pairs with different counting rates and average path lengths. Penetrating particles are measured by requiring signals in all 10 detectors.

MATERIALS AND METHODS

Figure 3 shows time-resolved measurements acquired by LND from 3 January to 12 January and from 31 January to 10 February 2019, i.e., when the lander was not hibernating during the intensely cold lunar night. To survive this extreme thermal environment, the Chang'E 4 lander contains a radioisotope thermoelectric generator (RTG) and three radioisotope heater units (RHUs); in addition, the Yutu-2 rover is also equipped with an RTG. We have measured the contributions of the lander RTG and RHUs in August 2018 before the launch of the spacecraft and have thus determined their contribution to be 5.2 ± 0.6 μGy/hour to the total dose rate and 1.7 ± 0.4 μGy/hour to the neutral dose rate (*20*). These values have been subtracted from the measurements shown in Fig. 3, which shows (from top to bottom) (A) the evolution of total dose rate with time and the same for neutral dose rate (B) and charged-particle dose rate (C), as well as the flux of penetrating particles (D). The first four data points in Fig. 3A lie above the remaining data points because they were acquired while the Yutu-2 rover with its RTG was still piggybacked on the lander deck. The following data points show the dose rate after the rover had rolled off the lander and was separated from the lander and LND by at least 7 m. The last 11 hours in the first lunar day show a further decrease in dose rate that also extends to 3 February 2019. During this period of time, the liquid NH_3 thermal control system (TCS; shown in red in inset A to Fig. 2) of the lander had been activated, provided additional shielding, and

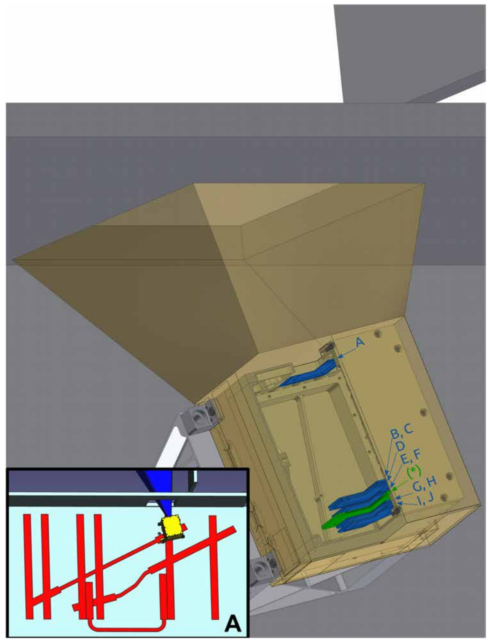

Fig. 2. Schematic view of the LND sensor head and its accommodation in the Chang'E 4 payload compartment. The LND detector system consists of 10 dual-segment silicon SSDs (A to J) shown and labeled in blue. They are arranged such as to form a particle telescope that views the sky through an opening of the payload compartment. The structure shown in green absorbs thermal neutrons and is irrelevant for this paper. This opening in the payload compartment (indicated by gray walls) is closed during the lunar night and reopened in the lunar morning. Multilayer insulation is shown in gold and insulates the LND sensor head, which is mounted to the side panel of the payload compartment with an Al bracket also shown in gray. Inset A shows LND's location on the payload panel (in pale blue) together with its NH_3 thermal control system (TCS) indicated in red.

modulated high-energy neutrons (*21*). The contribution of (predominantly) high-energy neutrons is shown in Fig. 3B and clearly exhibits a drop at the end of the first lunar day, which also extends throughout the time period when the TCS was active. As expected, the dose rate from charged particles (shown in Fig. 3C) shows no

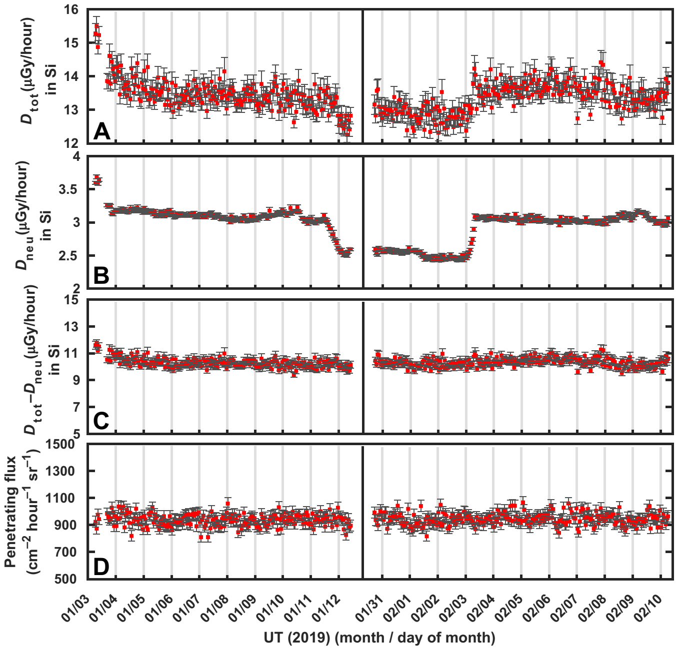

Fig. 3. Temporal evolution of the radiation environment on the Moon as measured by LND on Chang'E 4 during the first and second lunar day after Chang'E4 landed. The left-hand panels show data for the first lunar day, and the right-hand panels show data for the second lunar day. (**A**) Total absorbed dose rate measured with the LND B detector. (**B**) Neutral particle dose rate recorded in the LND C1 silicon detector. (**C**) Total absorbed dose rate from charged particles only [i.e., (A and B)]. The known background from the RTG and RHUs (*20*) has been subtracted from the values reported in (A) and (B). (**D**) Temporal evolution of the flux of penetrating particles. UT, universal time.

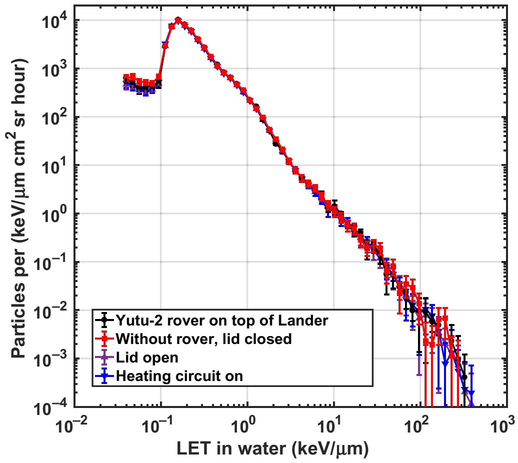

Fig. 4. Linear Energy Transfer (LET) spectra (converted to LET in water) measured during four different time periods show only small variations. The data shown as black circles were acquired before lander and rover separation; data shown in red after the rover left the lander but with the lid still closed; data in purple: normal operation of LND with the lid open; data in blue: with the Chang'E 4 heater circuit activated toward the end of the lunar day.

cotemporal decrease, nor does the flux of penetrating particles (Fig. 3D). The dose rates shown in Fig. 3 (A and C), as well as the flux of penetrating particles (Fig. 3D), show much larger fluctuations than the dose rate from neutral particles shown in Fig. 3B. This measurement primarily records the recoil energy transferred by neutrons to the Si nuclei of the C1 detector segment and the energy deposited by low-energy ($E_\gamma < 1$ MeV) γ rays. Because there is no directional information, the geometric factor for this measurement is much larger than that for penetrating particles. The fluctuations seen in Fig. 3 (A, C, and D) are thus due to statistical fluctuations and to fluctuations in the number of helium nuclei contributing to the total dose rate and even rarer contributions from heavy ions. The lander was again put into hibernation on 10 February 2019.

The LND measures time-resolved LET spectra that are remarkably invariant. Figure 4 shows such spectra acquired during the first lunar day. The black curve (black circles) shows the LET spectrum for the time period when the rover was still piggybacked on the lander, the red curve (and red squares) shows the same quantity while the lid that protects the LND sensor head from the cold night was still closed, and the purple upward triangles show data with the lid opened (as in Fig. 1). Last, the blue downward triangles show the LET spectrum acquired while the TCS was active. It is nearly impossible to distinguish any differences in these spectra. LET spectra are only measured for charged particles, so their invariance is consistent with the finding from Fig. 3 (C and D) that the charged particle dose rate and flux hardly varied at all during the LND measurements. Thus, the clear differences in measured dose rates seen in the course of the first two lunar days must be due to changes in the dose rate from neutral particles, which is also borne out by Fig. 3B and underlines the importance of also measuring the dose rate from neutral particles.

RESULTS

Ignoring the data acquired while Yutu-2 was still piggybacked on the lunar lander module and while the TCS was active [11 January 2019 (14:41) to 3 February 2019 (07:53)], we measured an average total dose rate in silicon of 13.2 ± 1 and 3.1 ± 0.5 µGy/hour in silicon for neutral particles. The background due to the RTG and RHUs was measured in August 2018 (*20*), and the values reported above have been corrected accordingly; the corresponding errors are reported separately in Table 1. Thus, we find that neutral particles contributed a nonnegligible fraction of 23 ± 8% to the total dose (*22*). Subtracting the neutral contribution, we find that the average absorbed dose rate due to charged particles is 10.2 ± 1.1 µGy/hour in Si. After conversion of the LET spectrum to LET in water, as discussed in Introduction, we obtain an average quality factor of $\langle Q \rangle = 4.3 \pm 0.7$. After multiplication of the charged-particle absorbed dose rate (in water) measurement given above with $\langle Q \rangle$, we obtain the GCR dose equivalent rate of 57.1 ± 10.6 µSv/hour from charged particles. A summary of the values discussed in this paragraph is given in Table 1.

While we can model the shielding provided by the LND instrument itself, the shielding provided by the lander (Fig. 1) is not known to us. LND is mounted to the inside panel of the Chang'E 4 payload compartment (shown in gray in Fig. 2). We estimate that most of the lander structure consists of honeycomb structures with an effective thickness corresponding to 1 mm of Al. The Al housing of the LND sensor head itself was milled to a thickness of 1.5 mm. Accounting for additional materials such as printed circuit boards in the sensor head and projection effects with a factor of square root of 2, we arrive at an average shielding thickness of ~3.5 mm Al equivalent. This corresponds to a shielding of ~1 g/cm^2 that can be compared to

Table 1. Summary of measurements of the radiation dose rate measured in μGy/hour on the lunar surface. The errors of the background dose rate from the RTG/RHUs (*20*) are considered systematic errors and have been added quadratically when reporting the final values in the rightmost column.

Dose rate (μGy/hour)	Measured	Background	Final in Si
Total	18.4 ± 0.4	5.2 ± 0.6	13.2 ± 0.7
Neutral	4.7 ± 0.1	1.7 ± 0.5	3.1 ± 0.5
Charged	13.7 ± 0.4	3.5 ± 0.8	10.2 ± 0.9

typical shielding values for extravehicular activities (EVAs) discussed, e.g., in (*23*), of 0.3 g/cm^2 of space suit fabric and 1 g/cm^2 for a pressurized rover vessel. Thus, the values reported here can be taken as good estimates for the dose rate during EVAs on the lunar surface.

Interpretation

To put the values reported here into context, we briefly summarize measurements by the Cosmic Ray Telescope for the Effects of Radiation (CRaTER) on Lunar Reconnaissance Orbiter (LRO) (*24*). Incidentally, LRO flew over the location of Chang'E 4 at 01:30 on 2 February 2019. At this time, both LND and CRaTER saw identical heliospheric conditions, and CRaTER measured a dose rate of 13.29 μGy/hour (reported by the CRaTER team as converted to water and to the lunar surface) with its D1 and D2 detectors (*25*) while LND measured a dose rate of 10.2 ± 1.1 μGy/hour in silicon (13.2 ± 1.4 μGy/hour converted to water) for charged particles (*26*). CRaTER uses a factor of 1.33 to convert dose rate from Si to water (*27*); therefore, it is more convenient to compare the dose rate measured in Si by LND (10.2 ± 1.1 μGy/hour) and CRaTER (10.0 μGy/hour). These two values are equal within uncertainties. Thus, the differences in shielding by the instruments themselves and the two spacecraft (*28*) have no noticeable effect on their measured dose rates.

DISCUSSION

LND measured an average dose equivalent of 1369 μSv/day on the surface of the Moon. For the same time period, the dose equivalent onboard the International Space Station (ISS) as measured with the DOSIS 3D DOSTEL instruments (*29*) was 731 μSv/day with contributions only from GCR of 523 μSv/day. The additional ~208 μSv/day is due to protons while crossing the South Atlantic Anomaly. Therefore, the daily GCR dose equivalent on the surface of the Moon is around a factor of 2.6 higher than the dose inside the ISS. Because the Sun is currently still in an extended activity minimum (*30*), the dose rate from GCR reported here may be considered as an upper limit for human exploration of the Moon during conditions of low solar activity. Settlements on the Moon will provide additional shielding because they will be buried beneath layers of lunar regolith. While this would decrease the dose rate from charged particles, the absolute contribution from neutrons is expected to increase for shielding constructed from in situ resources, as borne out by measurements with the Apollo 17 Lunar Neutron Probe Experiment. These showed that the flux of thermal and epithermal neutrons increases significantly up to a depth of approximately 150 g/cm^2 (*31*).

LND measured the radiation environment on the surface of the Moon at this precision for the first time. In addition, due to the fact that we are now approaching solar minimum conditions, the contributions from GCR can be seen as upper estimations for the GCR dose. In the time period reported here, no SPE was observed from the surface of the Moon. Such events can increase the dose by orders of magnitude behind only thin shielding (*32*).

REFERENCES AND NOTES

1. Task Group on Radiation Protection in Space; ICRP Committee 2, G. Dietze, D. T. Bartlett, D. A. Cool, F. A. Cucinotta, X. Jia, I. R. McAulay, M. Pelliccioni, V. Petrov, G. Reitz, T. Sato, ICRP, 123. Assessment of radiation exposure of astronauts in space. ICRP Publication 123. *Ann. ICRP* **42**, 1–339 (2013).
2. NASA, Space Radiation Cancer Risk Projections and Uncertainties – 2012 *Rep. NASA-STD-3001, VOLUME 1*, (2013).
3. U. Straube, T. Berger, G. Reitz, R. Facius, C. Fuglesang, T. Reiter, V. Damann, M. Tognini, Operational radiation protection for astronauts and cosmonauts and correlated activities of ESA Medical Operations. *Acta Astronaut.* **66**, 963–973 (2010).
4. F. A. Cucinotta, F. K. Manuel, J. Jones, G. Iszard, J. Murrey, B. Djojonegro, M. Wear, Space radiation and cataracts in astronauts, *Radiat. Res.* **156** (5 Pt. 1), 460–466 (2001).
5. P. Y. Chang, F. A. Cucinotta, K. A. Bjornstad, J. Bakke, C. J. Rosen, N. Du, D. G. Fairchild, E. Cacao, E. A. Blakely, Harderian gland tumorigenesis: Low-dose and LET response. *Radiat. Res.* **185**, 449–460 (2016).
6. D. M. Sridharan, A. Asaithamby, S. M. Bailey, S. V. Costes, P. W. Doetsch, W. S. Dynan, A. Kronenberg, K. N. Rithidech, J. Saha, A. M. Snijders, E. Werner, C. Wiese, F. A. Cucinotta, J. M. Pluth, Understanding cancer development processes after HZE-particle exposure: Roles of ROS, DNA damage repair and inflammation. *Radiat. Res.* **183**, 1–26 (2015).
7. F. A. Cucinotta, Review of NASA approach to space radiation risk assessments for Mars exploration. *Health Phys.* **108**, 131–142 (2015).
8. R. Jandial, R. Hoshide, J. D. Waters, C. L. Limoli, Space-brain: The negative effects of space exposure on the central nervous system. *Surg. Neurol. Int.* **9**, 9 (2018).
9. R. L. Hughson, A. Helm, M. Durante, Heart in space: Effect of the extraterrestrial environment on the cardiovascular system. *Nat. Rev. Cardiol.* **15**, 167–180 (2018).
10. G. A. Nelson, Space radiation and human exposures, a primer. *Radiat. Res.* **185**, 349–358 (2016).
11. L. W. Townsend, J. H. Adams, S. R. Blattnig, M. S. Clowdsley, D. J. Fry, I. Jun, C. D. McLeod, J. I. Minow, D. F. Moore, J. W. Norbury, R. B. Norman, D. V. Reames, N. A. Schwadron, E. J. Semones, R. C. Singleterry, T. C. Slaba, C. M. Werneth, M. A. Xapsos, Solar particle event storm shelter requirements for missions beyond low Earth orbit. *Life Sci. Space Res.* **17**, 32–39 (2018).
12. J. A. Simpson, Elemental and isotopic composition of the galactic cosmic rays. *Annu. Rev. Nucl. Part. Sci.* **33**, 323–382 (1983).
13. National Research Council 1996. Radiation Hazards to Crews of Interplanetary Missions: Biological Issues and Research Strategies. Washington, DC: The National Academies Press. https://doi.org/10.17226/5540.
14. F. A. Cucinotta, M. Durante, Cancer risk from exposure to galactic cosmic rays: Implications for space exploration by human beings. *Lancet Oncol.* **7**, 431–435 (2006).
15. R. A. English, R. E. Bensotz, J. Vernon Builey, C. M. Barnes, Apollo Experience Report—Protection against radiation, NASA Technical Note NASA TN D-7080 Retrieved from: https://ntrs.nasa.gov/archive/nasa/casi.ntrs.nasa.gov/19730010172.pdf.
16. The Apollo Lunar-Surface Experiments Package [ALSEP; (*33*)] provided time-resolved measurements of suprathermal ions (*34*) and charged particles (*35*) from Earth's magnetosphere and sheath, but this is unimportant for dosimetric purposes as the measured particles have insufficient energy to penetrate even the outermost layers of a space suit.
17. ICRP, 1990 Recommendations of the International Commission on Radiological Protection, ICRP Publication 60. *Ann. ICRP* **21**, 1–3 (1991).
18. C. Zeitlin, L. Narici, R. R. Rios, A. Rizzo, N. Stoffle, D. M. Hassler, B. Ehresmann, R. F. Wimmer-Schweingruber, J. Guo, N. A. Schwadron, H. E. Spence, Comparisons of high-linear energy transfer spectra on the ISS and in deep space. *Space Weather* **17**, 396–418 (2019).
19. R. F. Wimmer-Schweingruber, J. Yu, S. I. Böttcher, S. Zhang, S. Burmeister, H. Lohf, J. Guo, Z. Xu, B. Schuster, L. Seimetz, Johan L. Freiherr von Forstner, A. Ravanbakhsh, V. Knierim, S. Kolbe, H. Woyciechowsky, S. R. Kulkarni, B. Yuan, G. Shen, C. Wang, Z. Chang, T. Berger, C. E. Hellweg, D. Matthiä, D. Hou, A. Knappmann, C. Büschel, X. Hou, B. Ren, Q. Fu, The Lunar Lander Neutron and Dosimetry (LND) Experiment on Chang'E 4. *Space Sci. Rev.* **216**, 104 (2020). https://doi.org/10.1007/s11214-020-00725-3.
20. D. Hou, S. Zhang, J. Yu, R. F. Wimmer-Schweingruber, S. Burmeister, H. Lohf, B. Yuan, G. Shen, C. Wang, X. Hou, B. Ren, Removing the Dose Background from Radioactive Sources from Active Dose Rate Measurements in the Lunar Lander Neutron & Dosimetry

(LND) Experiment on Chang'E 4, J. Instrumentation, 15(1), P01023–P01032 (2020), https://doi.org/10.1088/1748-0221/15/01/P01032. The background measurements were performed separately for the RTG and all RHUs. This does not account for the possibility of neutron multiplication (*36*) in which neutrons from one RHU lead to nuclear reactions in another RHU and thus enhance the neutral radiation.
21. The Chang'E 4 payload thermal control system (TCS) circulates ammonia (NH_3) from the warm regions in the lander to the walls of the payload compartment where it provides heat during the late lunar evening, night, and early morning. During lunar daytime, the TCS that serves the payload compartment is empty. Six heat pipes service the panel to which LND is mounted. They are indicated in red in inset A of Fig. 2, where LND is shown in yellow.
22. The remarkably high dose rate from neutral particles reported here may be at least partially explained by neutron multiplication (*36*) and the production of secondary particles by the interaction of the GCR with the structure of the Chang'E 4 lander and LND.
23. J. W. Wilson, B. M. Anderson, F. A. Cucinotta, J. Ware, C. J. Zeitlin, Spacesuit Radiation Shield Design Methods, SAE Report 2006-01-2110, (2006).
24. H. E. Spence and Crater Science Team, An Overview of Results from the Lunar Reconnaissance Orbiter (LRO) Cosmic Ray Telescope for the Effects of Radiation (CRaTER), in *Annual Meeting of the Lunar Exploration Analysis Group*, LPI Contributions, **1595**, 66 (2010).
25. The effect of the varying distance on the effective shielding by the Moon is included in the dose rates published by the CRaTER team, as discussed on their website (http://prediccs.sr.unh.edu/craterweb/algorithms.html).
26. LND measures total dose and dose from neutral particles separately. The charged-particle dose is calculated as the difference.
27. N. A. Schwadron, T. Baker, B. Blake, A. W. Case, J. F. Cooper, M. Golightly, A. Jordan, C. Joyce, J. Kasper, K. Kozarev, J. Mislinski, J. Mazur, A. Posner, O. Rother, S. Smith, H. E. Spence, L. W. Townsend, J. Wilson, C. Zeitlin, Lunar radiation environment and space weathering from the Cosmic Ray Telescope for the Effects of Radiation (CRaTER). *J. Geophys. Res.* **117**, E00H13 (2012).
28. LND's B detector sees varying amounts of shielding because of its location inside LND and the Chang'E 4 lander; the minimum shielding is 25 μm of Al, 50 μm of Kapton, and 0.5 mm of Si. The CRaTER D1 and D2 detectors are also shielded by varying material thicknesses from the instrument and LRO spacecraft (*19*). If used in coincidence with other detectors, CRaTER's 148-μm D1 detector is shielded by a 0.82-mm-thick Al entrance window, and its 1-mm-thick D2 detector is thus shielded by 0.82 mm of Al and 148 μm of Si.
29. T. Berger, S. Burmeister, D. Matthiä, B. Przybyla, G. Reitz, P. Bilski, M. Hajek, L. Sihver, J. Szabo, I. Ambrozova, F. Vanhavere, R. Gaza, E. Semones, E. G. Yukihara, E. R. Benton, Y. Uchihori, S. Kodaira, H. Kitamura, M. Boehme, DOSIS & DOSIS 3D: Radiation measurements with the DOSTEL instruments onboard the Columbus Laboratory of the ISS in the years 2009–2016. *J. Space Weather Space Clim.* **7**, A08 (2017).
30. B. Kakad, A. Kakad, D. S. Ramesh, G. S. Lakhina, Diminishing activity of recent solar cycles (22–24) and their impact on geospace. *J. Space Weather Space Clim.* **9**, A1 (2019).
31. D. S. Woolum, D. S. Burnett, M. Furst, J. R. Weiss, Measurement of the lunar neutron density profile. *Moon* **12**, 231–250 (1975).
32. N. A. Schwadron, F. Rahmanifard, J. Wilson, A. P. Jordan, H. E. Spence, C. J. Joyce, J. B. Blake, A. W. Case, W. de Wet, W. M. Farrell, J. C. Kasper, M. D. Looper, N. Lugaz, L. Mays, J. E. Mazur, J. Niehof, N. Petro, C. W. Smith, L. W. Townsend, R. Winslow, C. Zeitlin, Update on the worsening particle radiation environment observed by CRaTER and implications for future human deep-space exploration. *Space Weather* **16**, 289–303 (2018).
33. Apollo 14 Preliminary Science Report, NASA, Special Publication SP-272 (1971).
34. H. K. Hills, J. W. Freeman Jr., Suprathermal Ion Detector Experiment (Lunar Ionosphere Detector), Charged-Particle Lunar Environment Experiment, in Apollo 14 Preliminary Science Report, NASA, Special Publication SP-272 (1971), pp. 175–183.
35. B. J. O'Brien, D. L. Reasoner, Charged-Particle Lunar Environment Experiment, in Apollo 14 Preliminary Science Report, NASA, Special Publication SP-272 (1971), pp. 193–213.
36. M. Taherzadeh, Neutron Radiation Characteristics of Plutonium Dioxide Fuel, Technical Report 32-1555, Revision 1, Jet Propulsion Laboratory, California Institute of Technology, Pasadena, California, December 1, (1972).

Acknowledgments: We thank the following facilities and personnel for supporting the calibration of LND: CERN/CERF in Geneva, Switzerland; NIRS, HIMAC in Chiba, Japan; ATI in Vienna, Austria; SFE at NSSC China. We thank the Lunar Exploration and Space Engineering Center and O. Angerer from DLR, Germany, for their unwavering support of Chang'E 4 and the China National Space Administration (CNSA) for data acquisition and dissemination. **Funding:** The work reported in this paper is supported by the Beijing Municipal Science and Technology Commission, grant no. Z181100002918003, and by NSFC grant no. 41941001. The work at USTC Hefei is partly supported by the Key Research Program of the Chinese Academy of Sciences (grant nos. XDPB11 and XDB41000000). The LND instrument is supported by the German Space Agency, DLR, and its Space Administration under grant 50 JR 1604 to the Christian-Albrechts-University (CAU) Kiel. **Author contributions:** S.Z., R.F.W.-S., S.B., H.L., T.B., J.G., C.E.H., and D.M. wrote the paper; J.Y., D.H., J.G., Z.X., J.L.F.v.F., and Chunqin Wang performed data analysis; S.B., J.Y., R.F.W.-S., S.Z., X.H., J.C., and S.R.K. calibrated LND; R.F.W.-S., S.I.B., L.S., B.S., V.K., and J.Y. designed LND; S.Z., Chi Wang, Q.F., Y.Z., Y.S., C.X., J.L., Z.Z., H.Z., Z.C., B.Z., Y.C., H.G., G.S., B.Y., H.X., and Z.Q. were responsible for managing interfaces and instrument performance on the Chinese side. Thus, all authors contributed equally. **Competing interests:** The authors declare that they have no competing interests. **Data and materials availability:** The data used in this report are being made available by the Chinese Lunar Exploration Space Engineering Center (LESEC) at their website http://moon.bao.ac.cn/index_en.jsp. All data needed to evaluate the conclusions in the paper are available at Dryad under doi: 10.5061/dryad.7h44j0zs1. Additional data related to this paper may be requested from the first author (S.Z.).

Submitted 14 August 2019
Accepted 12 August 2020
Published 25 September 2020
10.1126/sciadv.aaz1334

Citation: S. Zhang, R. F. Wimmer-Schweingruber, J. Yu, C. Wang, Q. Fu, Y. Zou, Y. Sun, C. Wang, D. Hou, S. I. Böttcher, S. Burmeister, L. Seimetz, B. Schuster, V. Knierim, G. Shen, B. Yuan, H. Lohf, J. Guo, Z. Xu, J. L. Freiherr von Forstner, S. R. Kulkarni, H. Xu, C. Xue, J. Li, Z. Zhang, H. Zhang, T. Berger, D. Matthiä, C. E. Hellweg, X. Hou, J. Cao, Z. Chang, B. Zhang, Y. Chen, H. Geng, Z. Quan, First measurements of the radiation dose on the lunar surface. *Sci. Adv.* **6**, eaaz1334 (2020).

Science Advances

First measurements of the radiation dose on the lunar surface

Shenyi Zhang, Robert F. Wimmer-Schweingruber, Jia Yu, Chi Wang, Qiang Fu, Yongliao Zou, Yueqiang Sun, Chunqin Wang, Donghui Hou, Stephan I. Böttcher, Sönke Burmeister, Lars Seimetz, Björn Schuster, Violetta Knierim, Guohong Shen, Bin Yuan, Henning Lohf, Jingnan Guo, Zigong Xu, Johan L. Freiherr von Forstner, Shrinivasrao R. Kulkarni, Haitao Xu, Changbin Xue, Jun Li, Zhe Zhang, He Zhang, Thomas Berger, Daniel Matthiä, Christine E. Hellweg, Xufeng Hou, Jinbin Cao, Zhen Chang, Binquan Zhang, Yuesong Chen, Hao Geng and Zida Quan

Sci Adv **6** (39), eaaz1334.
DOI: 10.1126/sciadv.aaz1334

Science Advances (ISSN 2375-2548) is published by the American Association for the Advancement of Science, 1200 New York Avenue NW, Washington, DC 20005. The title *Science Advances* is a registered trademark of AAAS.